An analysis of frequency response on OLED for lighting applications

Nórton D. Barth
GEDRE - Intelligence in Lighting
Federal University of
Santa Maria (UFSM)
Santa Maria- Brazil
norton@gedre.ufsm.br

Vitor C. Bender
Group of Integrated Exploration
Energy Resources (EIRE)
Federal University of Pampa (UNIPAMPA)
Alegrete - Brazil
vitorbender@unipampa.edu.br

Tiago B. Marchesan
GEDRE- Intelligence in Lighting
Federal University of
Santa Maria (UFSM)
Santa Maria- Brazil
tiago@ufsm.br

Abstract—**Organic light-emitting diodes (OLEDs) are a new technology with great potential for lighting applications. They have a large area providing a comfortable light and a good thermal dissipation. Once the OLEDs applications in lighting are recently, is necessary to create an electrical equivalent model for their analysis, because this knowledge is requested to improve the performance of the lighting systems. This paper will show an analysis based on datasheet information and computer simulation to approach OLED electrical performance including the luminance behavior.**

Index Terms—**OLEDs, Dynamic Model, Dimming, Pulse frequency modulation**

I. INTRODUCTION

The energy consumption has been steadily rising, therefore developing more efficient equipment are necessary. In USA, the energy spent on lighting represent 10% of the residential consumption [1]. OLEDs start to be a new technology in light after the creation of the first white light OLED, by the mixing of different colors emitters [2]. Once the OLEDs are thin, could be mirror or transparent and have a large area, they start to be a good choice for decorative and architecture application [3].

OLED luminous efficacy still far in comparison to the other light sources and will request more time to achieve a high efficacy [4], is necessary improve the knowledge about this light system to development drive circuits.

This paper will show a methodology that analyses the dynamic of a photo-electric equivalent model and after that analyze the frequency response and behavior of the voltage and light when using a current source.

II. OLED DYNAMIC CHARACTERIZATION

The simple structure of an OLED composed by the deposit of organic layers between a transparent electrode and a reflective metal, in order to create the anode and cathode, respectively. When applied a DC signal, the OLED characteristic I-V is similar to the inorganic LED (light-emitting diode). Several electrical equivalent circuits were proposed in order to represent the device behavior [5] [6], [7], but in this paper will be used the model shown in Fig. 1-a [3]. This model represent accuracy for frequencies lower than a decade below the light
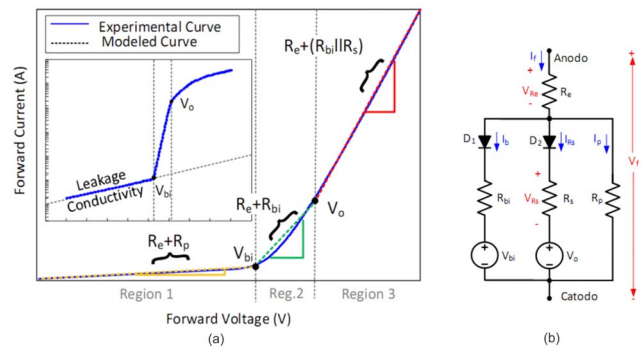

Fig. 1: (a) I-V curve for OLEDs
(b) Small-signal OLED equivalent circuit

cut-off frequency. The light cut-off frequency will be explained later in this paper.

The I-V curve of OLEDs represented in Fig. 1-b can be described for three regions. Region 1 , represents the leakage current that flows throught the resistor R_p and the resistor (R_e) created by an electrode. Region 2, represents when the current increase but the OLED stay do not emitting light. During this stage the current is limited by the R_e and the built-in resistor R_{bi}. The Region represent the static OLED model when the device start to produce light, in this case, the current flows in R_e and then is divided between R_{bi} and the series resistor R_s that act similar to inorganic LEDs. In the electrical equivalent model for OLEDs the voltages V_o and V_{bi} have the function of enable or disable each stage, represented by each circuit branch.

For a dynamic analysis is important to include the effect of OLED capacitance created by the large area and staked structure of the device, such capacitance is named geometrical capacitance (C_g) and the recombination of carriers in OLED layers creates a diffusion capacitance C_d [8]. With all this consideration, it is possible to create an electrical-dynamic model for OLEDs, as show Fig. 2.

Analyzing the circuit of Fig. 2, it is possible to divide the OLED operation in six stages when applied a current that will be I_f during $(0 < t < dT)$ and 0A for $(dT < t < T)$ where d is the duty cycle and T the period.
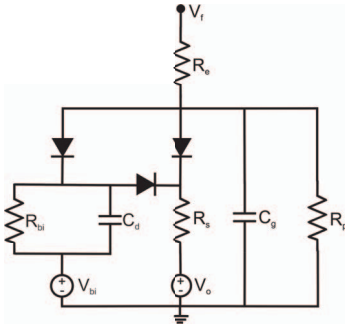
Fig. 2: OLED dynamical electrical model

A. Initial charge stage

The initial charge on Fig. 3, is active during the period when the OLED voltage $(V_f(t))$ is between $(0 < V_f < V_{st2})$, once V_{st2} represent the maximum voltage for this period (1). This stage the current flow through the resistor R_e and charge C_g, a small current circulates by R_p. This stage can be represented by (2) and (3).

$$V_{st2} = V_{bi} + I_f \cdot R_e \tag{1}$$

$$\tau_1 = \frac{1}{C_g \cdot R_p} \tag{2}$$

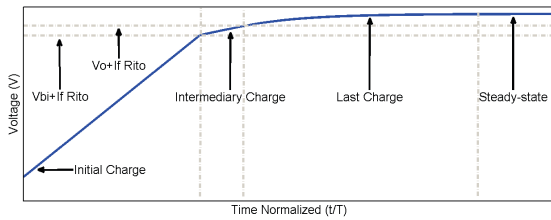$$V_f(t) = I_f \cdot R_e + I_f \cdot R_p(1 - e^{-t \cdot \tau_1}) \tag{3}$$

Fig. 3: Charge Characteristics

Equation (3) shows that when applied a current square wave, V_f do a step with the magnitude equals $(I_f \cdot R_e)$ and after that increase by a relation between current and the geometrical capacitance. In this stage OLED do not produce light.

B. Intermediary charge stage

The intermediary charge represented on Fig. 3, during the period when $(V_{st2} < V_f(t) < V_{st3})$, as a result the current flows trough R_e and charge C_g and C_d, a part of current flows trough R_{bi} and R_p. Regarding the current that flows for R_{bi} is larger than R_p, because R_p is at list a thousand times large than R_{bi}. The equations (1) and (4) represent the limit voltage for this stage, additionally the equations (5) and (6) represent the OLED behavior.

$$V_{st3} = V_o + I_f \cdot R_e \tag{4}$$

$$\tau_2 = \frac{R_p \cdot R_{bi}}{(R_p + R_{bi}) \cdot (C_d + C_g)} \tag{5}$$

$$V_f(t) = V_{st2} + \left[\left(I_f + \frac{V_{bi}}{R_{bi}} \right) \left(\frac{R_{bi} \cdot R_p}{R_{bi} + R_p} \right) - V_{bi} \right] \cdot (1 - e^{-t \cdot \tau_2}) \tag{6}$$

This stage ends when the capacitor C_g have a voltage equals to V_o.

C. Last charge stage

The last charge stage represents when the OLED start to emit light. This period is active for $(V_{st3} < V_f(t))$ and $(0 < t < dT)$. During this period the most part of current flows for R_s, this current is a mirror of the light emitted by OLEDs [9]. This stage can be represent by (4), (7) and (8).

$$\tau_3 = \frac{1}{\dfrac{Cd + Cg}{\dfrac{1}{R_p} + \dfrac{1}{R_s} + \dfrac{1}{R_{bi}}}} \tag{7}$$

$$V_f(t) = V_{st3} + \left(\frac{\dfrac{V_{bi}}{R_{bi}} + \dfrac{V_o}{R_s} + I_f}{\dfrac{1}{R_s} + \dfrac{1}{R_{bi}} + \dfrac{1}{R_p}} - V_o \right) (1 - e^{-t \cdot \tau_3}) \tag{8}$$

The equation (8) represent the last charge after a period of time equals to 5τ when the transient effect will be minimum. Considering this case, it is possible to represent the OLED steady-state (9).

$$V_{fstdy} = V_{st3} + \frac{\dfrac{V_{bi}}{R_{bi}} + \dfrac{V_o}{R_s} + I_f}{\dfrac{1}{R_s} + \dfrac{1}{R_{bi}} + \dfrac{1}{R_p}} - V_o \tag{9}$$

Using the equation (8), is possible to determinate (10), who represent the current flowing throught R_S. For this stage, I_{R_s} represent the light emitted by the OLED (11).

$$I_{Rs} = \left(\frac{\dfrac{V_{bi}}{R_{bi}} + \dfrac{V_o}{R_s} + I_f}{\dfrac{1}{R_s} + \dfrac{1}{R_{bi}} + \dfrac{1}{R_p}} - V_o \right) \cdot \left(\frac{1 - e^{-t \cdot \tau_3}}{R_s} \right) \tag{10}$$

$$I_{Rs} = k_\phi \cdot \phi_{OLED} \tag{11}$$

In (10) the constant k_ϕ create a correlation between the light flux (ϕ_{OLED}) and the current I_{Rs}. At this point, all the behavior characteristics of OLED when the current I_f is applied was describe during this period $(0 < t < dT)$.

D. Initial discharge stage

This process starts when the current $I_f = 0A$ and continues till the end of cycle $dT < t < T$. This stage can be represented by (12). Regarding this equation V_{charge} is the voltage on OLED in the last moment before I_f. If the OLED achieve the steady-state voltage, V_{charge} will be equal to $V_{f_{stdy}}$. The discharge equations represent a summing of the all discharge effects.

$$V_f(t) = (V_{charge} - V_{st3})e^{-t \cdot \tau_3} + (V_o - V_{bi}) \cdot e^{-t \cdot \tau_2} + V_{bi} \cdot e^{-t \cdot \tau_1} \quad (12)$$
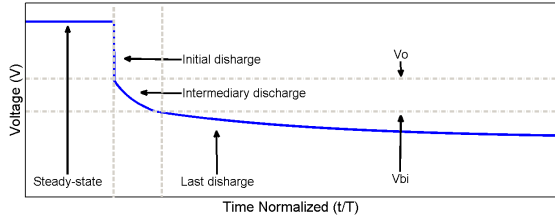

Fig. 4: Discharge characteristic

The equation (12) prove why the abrupt voltage fall appear on Fig. 4. This happen because the current is reduced to zero removing the drop voltage created by the current in R_e and after this point V_f is equals V_{Cg}. In the initial discharge the OLED still emitting light, the equation (13) show I_{Rs}, that could be related with the light equation (11).

$$I_{Rs} = \frac{(V_{charge} - V_{st3})e^{-t \cdot \tau_3} + (V_o - V_{bi}) \cdot e^{-t \cdot \tau_2} + V_{bi} \cdot e^{-t \cdot \tau_1}}{R_s}$$
$$(13)$$

This discharge ends when $(V_f < V_o)$ and at this point the OLED stop producing light, but the capacitors C_g and C_d still charged and the OLED will discharging until the cycle end.

E. Intermediary discharge stage

This discharge occurs for $(V_{bi} < V_f(t) < V_o)$, at the end of the stage, the capacitor C_d will be complete discharge over R_{bi} and just will rest C_g with charge.

$$V_f(t) = (V_o - V_{bi}) \cdot e^{-t \cdot \tau_2} + V_{bi} \cdot e^{-t \cdot \tau_1} \quad (14)$$

During the intermediary discharge the OLED will not produce light, once there is no current I_{Rs}.

F. Last discharge stage

This discharge will occur when just the capacitor C_g have a voltage lower than V_{bi}, and will discharge over R_p. This process will be shown by (15).

$$V_f(t) = V_{bi} \cdot e^{-t \cdot \tau_1} \quad (15)$$

This process will request a long time comparing to others stages, once the resistance R_p is at least a thousand times large than others resistances.

III. OLED RESPONSE FOR HIGH FREQUENCY

After this point is not necessary to observe the luminous flux dynamic once the human eye will not notice the transitory effects, so the analyse will just consider the average value [10] [11]. The equations (16) and (17) represents the OLED characteristics under frequencies a decade below the light cut-off frequency $(f_{c\phi})$. The $f_{c\phi}$ is similar to the cut off frequency in a high-pass filter, which represent a point from where the luminous flux decrease tightly in according with frequency decrease.

$$R_{eq} = R_s \cdot R_{bi} \cdot R_p \quad (16)$$

$$f_{c\phi} = \frac{R_p \cdot R_s + R_p \cdot R_{bi} + R_s \cdot R_{bi}}{(C_d + C_g) \cdot (R_p \cdot R_s \cdot R_{bi})} \cdot \frac{1}{2 \cdot \pi} \quad (17)$$

The OLED equivalent circuit under high frequencies still the same, but at this moment, is important to consider that the device will not discharge the capacitors, so the voltage V_{cg} will be at list V_o. Once the OLED still activated by the current square wave, the ϕ_{avg} can be represented by (18).

$$\phi_{avg}(s) = D \cdot \left(\frac{2 \cdot (V_o + V_{bi}) \cdot C_d \cdot C_g}{V_o \cdot (C_d + C_g)^2} \cdot \frac{s}{s + 2 \cdot \pi \cdot f_{c\phi}} + 1 \right)$$
$$(18)$$

The equation (18) is like the amplitude of the I_{Cg} and I_{Cd}. This characteristic shows that the luminous flux has a behavior similar to a high pass filter with a minimum value determined by the duty cycle of the current applied in OLED.

IV. EXPERIMENTAL RESULTS

After the process to modeling the dynamic characteristics of OLEDs, was created an algorithmic to reproduce the OLED response to a current square wave. For this analysis was utilized the OLED Philips GL-30, and the equivalent parameters are showing Table I [12].

TABLE I: OLEDs Parameters

Parameters	GL-30
$R_e (\Omega)$	1.523
$R_{bi} (\Omega)$	5.032
$R_s (\Omega)$	1.79
$R_p (M\Omega)$	10.6
$C_d (\mu F)$	1.329
$C_g (\mu F)$	0.494
$V_o (V)$	6.765
$V_{bi} (V)$	5.769

Using these parameters is possible to reproduce the response for the OLED in the first cycle and the response of the OLED in steady-state after many cycles. To confirm the steady-state in the algorithm was included a control loop that compare the voltage in different periods for errors lower than 0.1%. The step time using in the algorithm was 1ns for all frequencies. Fig. 5 and 6 represent the dynamic behavior in the first cycle (when the voltage starts in zero) for the OLED GL-30.
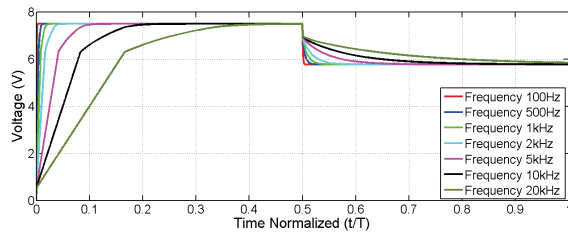
Fig. 5: OLED GL-30 voltage model behavior

The voltage response for the first cycle of a square wave current applied OLED GL-30 is represented in Fig. 5. This figure represent all stages previously explained and the different behaviors in relation to the frequency.
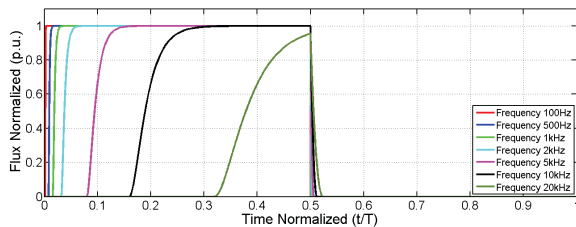

Fig. 6: OLED GL-30 light model behavior

Fig. 6 demonstrates that, once the frequency increase, the light decrease. This fact is wrong, because the OLED light intensity increase with high frequencies, so is important to use a high-frequency analyses for higher frequencies.

During the test was applied a square wave current $I_f = 350mA$ with an average value of 175mA and frequencies between 1kHz to 500kHz. With this configuration a photodiode was used to perform the light measurement . The experimental results are shown in fig 7, 8, 9, for 1kHz, 20kHz and 500kHz, respectively.
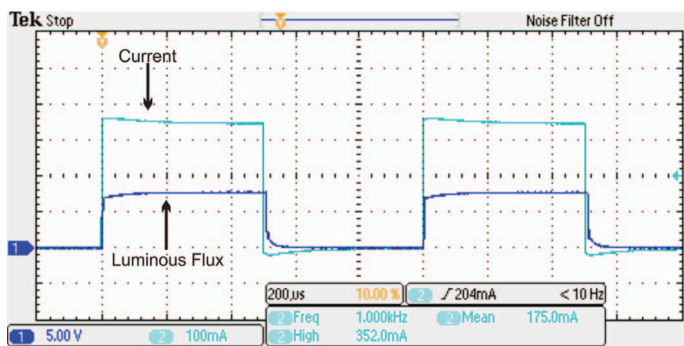

Fig. 7: OLED Response on 1kHz
CH1 - OLED light Output, 5V/div, 200 μs/div
CH2 - Current, 100mA/div, 200 μs/div

The Fig 7 show the light response for low frequency. Fig. 8 demonstrate that the low frequency equation not represent correctly, so is important use the analyses for the high frequency. The high-frequency method just return the average luminous
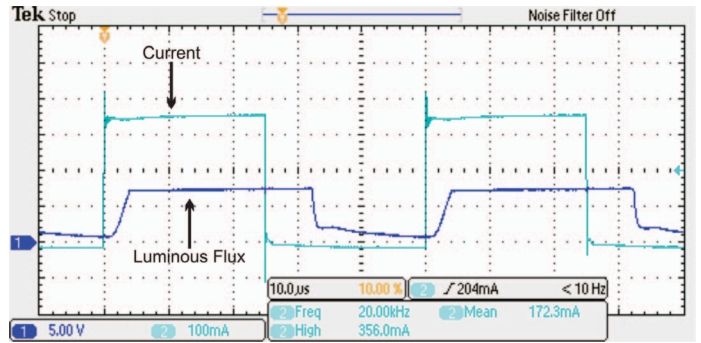

Fig. 8: OLED Response on 20kHz
CH1 - OLED light Output, 5V/div, 10 μs/div
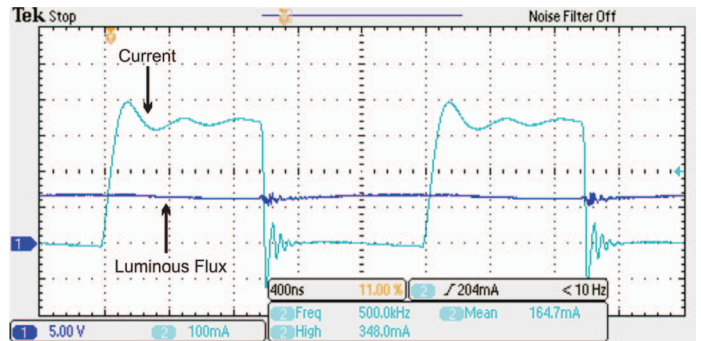CH2 - Current, 100mA/div, 10 μs/div

Fig. 9: OLED Response on 500kHz
CH1 - OLED light Output, 5V/div, 400ns/div
CH2 - Current, 100mA/div, 400ns/div

flux, but not the dynamic behavior. Fig. 9 demonstrate that the luminous flux is constant.
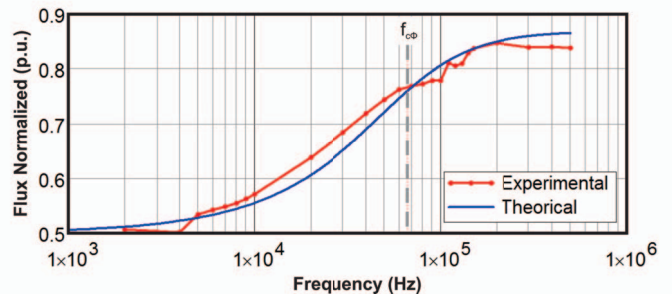

Fig. 10: Comparison between theoretical model, simulation and experimental results

After the experimental test, the data collected was analyzed to compare with a simulation and theoretical model (Fig. 10). Is important to observe that the experimental average OLED luminous flux have a high pass filter characteristic and can be represented by (18). The absolute error is demonstrate on fig (11), with the maximum error of 10.5% and an average error of 3.95%.
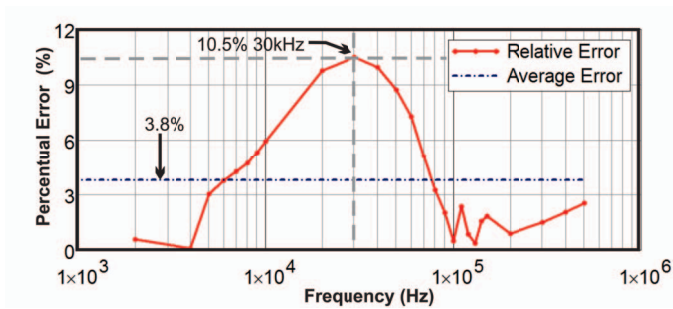
Fig. 11: Comparative error between experimental and theoric results

V. Conclusion

In this paper was shown the dynamic characteristic, creating a knowledge to project drive circuits for OLEDs application. The analysis shows each step for charge and discharge for low frequency, creating link with the voltage and the luminous flux. For high frequency, this paper show the behavior of the average luminous flux and way to reproduce on simulation this behavior.

The developed algorithm reproduces the response of simulator, with the purpose to compare the OLED luminous flux response in different frequencies with normalize time. In order to confirm the algorithm accuracy and validity, the response was compare with the simulator results.

Considering the light cut-off frequency location and the light characteristic response, is possible to project drive circuit to supply OLEDs without the output capacitor with the advantage to dimming the light and increase the efficiency of the OLED [4].

References

[1] U. E. I. A. EIA, "Anual energy outlook," 2016.
[2] J. Kido, M. Kimura, and K. Nagai, "Multilayer white light-emitting organic electroluminescent device," *Science*, vol. 267, no. 5202, p. 1332, 1995.
[3] V. C. Bender, N. D. Barth, R. A. Pinto, J. M. Alonso, and T. B. Marchesan, "Scale-photo-electro-thermal model for organic light-emitting diodes," *IET Optoelectronics*, vol. 10, no. 3, pp. 100–110, 2016.
[4] B. P. Z. Georges, *2014 Status Report on Organic Light Emitting Diodes (OLED)*. Publications Office of the European Union, 2014.
[5] J. P. Bender and J. F. Wager, "Alternating-current thin-film electroluminescent device modeling via spice fowler-nordheim diode," *IEEE Transactions on Electron Devices*, vol. 47, pp. 1113–1115, May 2000.
[6] C. Pinot, H. Cloarec, J.-C. Martinez, T. Maindron, D. Vaufrey, C. Prat, H. Doyeux, G. Haas, and Y. Bonnassieux, "P-157: Electrical modeling and numerical simulation of doped multilayer organic light-emitting diodes (oleds)," *SID Symposium Digest of Technical Papers*, vol. 38, no. 1, pp. 792–795, 2007.
[7] D. Buso, S. Bhosle, Y. Liu, M. Ternisien, C. Renaud, and Y. Chen, "Oled electrical equivalent device for driver topology design," *IEEE Transactions on Industry Applications*, vol. 50, no. 2, pp. 1459–1468, 2014.
[8] V. C. Bender, N. D. Barth, F. B. Mendes, R. A. Pinto, J. M. Alonso, and T. B. Marchesan, "Modeling and characterization of organic light-emitting diodes including capacitance effect," *IEEE Transactions on Electron Devices*, vol. 62, pp. 3314–3321, Oct 2015.
[9] R. L. Lin, J. Y. Tsai, D. Buso, and G. Zissis, "Oled equivalent circuit model with temperature coefficient and intrinsic capacitor," in *2014 IEEE Industry Application Society Annual Meeting*, pp. 1–8, Oct 2014.
[10] M. Perz, I. Vogels, D. Sekulovski, L. Wang, Y. Tu, and I. Heynderickx, "Modeling the visibility of the stroboscopic effect occurring in temporally modulated light systems," *Lighting Research & Technology*, vol. 47, no. 3, pp. 281–300, 2015.
[11] J. Bullough, K. S. Hickcox, T. Klein, A. Lok, and N. Narendran, "Assist recommends: Flicker parameters for reducing stroboscopic effect from solid-state lighting systems," 2011.
[12] V. C. Bender, N. D. Barth, M. Camponogara, R. A. Pinto, T. B. Marchesan, and J. M. Alonso, "Dynamic characterization and modeling of organic light-emitting diodes (oleds)," in *2015 IEEE Industry Applications Society Annual Meeting*, pp. 1–8, Oct 2015.